Science of the Total Environment 886 (2023) 163855

Contents lists available at ScienceDirect

Science of the Total Environment

journal homepage: www.elsevier.com/locate/scitotenv

An empirical and modelling approach to the evaluation of cruise ships' influence on air quality: The case of La Paz, Mexico

Osiel O. Mendoza-Lara [c], Claudia Yazmín Ortega-Montoya [b,*], Adria Imelda Prieto Hinojosa [a], Andrés Osvaldo López-Pérez [a], J.M. Baldasano [c]

[a] Tecnologico de Monterrey, Escuela de Ingeniería y Ciencias, Paseo del Tecnológico 751, 27250, Torreón, México
[b] Universidad Autónoma de Coahuila, Facultad de Ciencias Biológicas, Carretera Torreón-Matamoros Km. 7.5, 27276, Torreón, México
[c] Technical University of Catalonia (UPC), Barcelona Supercomputing Center (BSC), Avda. Diagonal 647, planta 10, 08028, Barcelona, Spain

HIGHLIGHTS

- Cruise ship's impact on air quality modelling (AERMOD-WRF).
- The spatial pattern of pollutant concentration using low-cost analysers.
- Differential Moran's I Index with local indicators of spatial association (DiLISA).
- The influence of multiple-source pollutants on air quality was elucidated using a hybrid methodology.

GRAPHICAL ABSTRACT

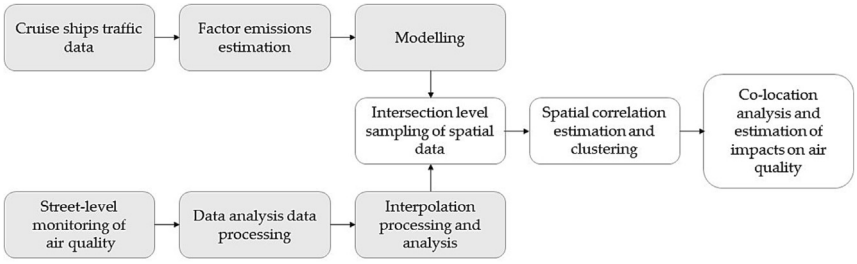

ARTICLE INFO

Editor: Pavlos Kassomenos

Keywords:
Air pollution
Modelling
Cruise ship
WRF-AERMOD
Differential Moran index
Radial basis function (RBF) interpolation

ABSTRACT

Maritime activity has diverse environmental consequences impacts in port areas, especially for air quality, and the post-COVID-19 cruise tourism market's potential to recover and grow is causing new environmental concerns in expanding port cities. This research proposes an empirical and modelling approach for the evaluation of cruise ships' influence on air quality concerning NO_2 and SO_2 in the city of La Paz (Mexico) using indirect measurements. EPA emission factors and the AERMOD modelling system coupled to WRF were used to model dispersions, while street-level mobile monitoring data of air quality from two days of 2018 were used and processed using a radial base function interpolator. The local differential Moran's Index was estimated at the intersection level using both datasets and a co-location clustering analysis was performed to address spatial constancy and to identify the pollution levels. The modelled results showed that cruise ships' impact on air quality had maximum values of 13.66 μg/m^3 for NO_2 and 15.71 μg/m^3 for SO_2, while background concentrations of 8.80 for NO_x and 0.05 for SO_x (μg/m^3) were found by analysing the LISA index values for intersections not influenced by port pollution. This paper brings insights to the use of hybrid methodologies as an approach to studying the influence of multiple-source pollutants on air quality in contexts totally devoid of environmental data.

1. Introduction

Cruise tourism is an important economic activity worldwide that generates over USD 150 billion every year (CLIA, 2020b). Defined as a mixture of maritime transport, travel and tourism services, cruise shipping offers passengers leisure activities that include onboard amenities, shore excursions and at least one night on board a seagoing vessel with a capacity of at least 100 passengers (Pallis, 2017). Before the COVID-19 pandemic that forced the sector to come to a 15-month standstill, cruise lines had sustained a continuous growth of 5.4 % in the period of 2009–2019 (CLIA, 2020a); the sustained growth of the sector is the result of the sector's transformation with increases in ship volume and passenger capacity, and some ships can currently accommodate 6000 passengers and crew

* Corresponding author.
E-mail address: yazmin.ortega@uadec.edu.mx (C.Y. Ortega-Montoya).

http://dx.doi.org/10.1016/j.scitotenv.2023.163855
Received 13 December 2022; Received in revised form 6 April 2023; Accepted 27 April 2023
Available online 2 May 2023

members combined, surpassing the number of residents in many small towns and villages (Stefanidaki and Lekakou, 2014).

In 2022, the cruise industry is projected to operate with 272 ships, where only three large companies, namely Carnival Corporation, Royal Caribbean Cruises and Norwegian Cruise Line, account for most of the market and represented 70.9 % of the total market in 2021 (Cruise Market Watch, 2022). The economic activity scenario's forecast for the end of 2026 estimates a passenger volume recovery and growth of 12 % above the 2019 levels (CLIA, 2022).

Even when new cruise ships are powered by LNG as a strategy from the sector to attend to sustainability concerns, most vessels use low-grade diesel with a high sulphur content as a result of marine fuel quality that tends to be less regulated and less refined than other types of fuel (Sarnelli, 2021). This low quality of diesel fuel justified the rule implemented by the International Maritime Organization (IMO) to reduce the sulphur content in marine fuels from 3.5 % to 0.5 % mass by mass (m/m) globally, beginning 1 January 2020 (IMO, 2020).

However environmental issues related to cruise ships are broader according to the work in (Lloret et al., 2021); this includes issues related to the air, water, soil and land cover, sensitive habitats and protected areas, onshore and marine wildlife, and waste disposal. In relation to impacts on the air, major pollutants of concern related to marine transport sources include sulphur oxides (SO_x), particulate matter (PM), oxides of nitrogen (NO_x), carbon monoxide (CO) and volatile organic compounds (VOCs); as well as the carbon dioxide (CO_2) emission, the main greenhouse gas.

Health effects related to air pollutants include acute exposure effects and long-term exposure effects. The acute effects of SO_2 in the air can cause breathing difficulties and asthma attacks, while the long-term effects include respiratory illness, aggravation of existing heart disease and premature death (Pan, 2011; WHO, 2016).

Exposure to fine particles can cause eye, nose, throat, and lung irritation and affect lung function and worsen asthma and heart disease, while long-term exposure to fine particulate matter may be associated with increased rates of chronic bronchitis, reduced lung function and increased mortality from lung cancer and heart disease (EPA, 2021a). $PM_{2.5}$ emissions from ships have shown the presence of compounds with potential health effects such as heavy metals, polycyclic aromatic hydrocarbons, dioxins/ furans, and black carbon (Anastasopolos et al., 2021). The $PM_{2.5}$ burden of mortality is related to cardiopulmonary and lung cancer deaths (Corbett et al., 2007).

Nitrogen oxides (NO_2) adverse health effects include the intensification of common viral infections and severe damage to the lungs as well as asthma (de Vries, 2021). Acute and chronic exposure to carbon monoxide is associated with an increased risk for adverse cardiopulmonary events, including death (Chen et al., 2007). Exposure to VOC can cause eye, nose and throat irritation and nausea, while long-term exposure can affect the liver, kidney and nervous system or cause cancer (EPA, 2021c).

Several investigations have found a direct correlation between air pollutants and cruise ships (Chatzinikolaou et al., 2015; Nguyen et al., 2022; Ruiz-Guerra et al., 2019), with the size and age of the cruise ship being important variables of the air emissions (Perdiguero and Sanz, 2020). Air pollutants' impact on health can also be economically quantified, and this was reported to reach or to EUR 5.3 per passenger in five Greek ports (Maragkogianni and Papaefthimiou, 2015) for NO_x, SO_2 and $PM_{2.5}$ emissions. In the Iberian Peninsula, the costs related to the health effects of PM, NO_2 and $PM_{2.5}$ were 0.72 %, 0.15 % and 0.28 % of the gross domestic product in 2015, respectively (Nunes et al., 2021).

In México in 2018, according to the Bank of Mexico, the cruise industry contributed USD 480 million (Nguyen et al., 2022). In the aftermath of COVID-19, the rebooting of the sector has created new routes to the main Mexican destinations (Garduño, 2021).

Emissions from maritime activity, as well as their impact on air quality, have been little analysed, especially in Mexico. However, only the estimation of emissions in the port of Veracruz has been carried out, as well as the proposal of the methodologies for its application.

Currently, only ship emissions have been estimated for some ports in Mexico (Fuentes García et al., 2021a, 2021b). Estimations of the impact on air quality due to emissions from maritime activity have been little analysed, especially in Mexico.

1.1. Area of study

The city of La Paz is the municipal seat of the municipality of the same name, as well as the capital of the state of Baja California Sur; it has a population of 250,141 and an urban extension of 78.58 km^2. The towns of El Centenario and Chamelita are also part of the same urban areas with a total of 9440 additional people around the bay of La Paz as well as three main ports: Pichilingue, Punta Prieta and La Paz ports. Among these three ports, only Pichilingue and La Paz are public; Punta Prieta's port is for exclusive governmental use and is where the electric power plant that supplies electricity to the city is located. Pichilingue is a deep-sea and cabotage port with ferry connections to the continental massif; it has a ferry terminal, customs facilities, two passenger terminals with the capacity to receive mega-cruises, a manoeuvring yard, warehouses, a commercial port, scales, and offices; additionally, it has the infrastructure for the shipment of bulk cement and the unloading and storage of LP gas.

Additionally, the port of La Paz is focused on tourism; it receives mainly yachts, medium-sized sailboats and boats for sport fishing; it has the capacity to receive boats with a maximum length of 65.5 m, width of 21.6 m and a maximum draft of 4.5 m. In addition, it has a dock for small boats and a tourist area. The city of La Paz in Mexico has special characteristics related to air quality that must be considered in order to fully understand the contexts of the present study:

1. The state of Baja California Sur has the highest rate of motorisation in Mexico due to its low population density and extreme weather conditions during most of the year, which disincentives alternative transportation modes (Islas-Rivera et al., 2011).
2. Two thermoelectric plants provide energy to the region because the regional grid is isolated from the national electric service; these are located in the La Paz Bay area and use high-sulphur-content fuel oil (Universidad Autónoma de Baja California Sur, 2016) as the main fuel for their operations.
3. The cargo and touristic activities in the port, which are expected to continue. Future trends are related to the construction of the biggest cruise terminal in the region to promote tourism activities in the area (Kalosh, 2021). This also is heavily influenced by the isolation of the region from the rest of the country, the long road distances through the Baja California Peninsula and the presence of deep-sea ports in the country due to the smaller distances by travel over water than by road.
4. While two air quality monitoring campaigns were carried out in La Paz in 2010 and 2014 by the Instituto Nacional de Ecología y Cambio Climático (INECC), only indicators were presented. The result of these campaigns showed that there are high concentrations of SO_2 at the site that coincide with the plume from the power plants and high concentrations of PM_{10} due to paved and unpaved roads, eroded soils, and other factors (INEGI, 2018); nevertheless, this report does not include port activities.
5. Currently, the city of La Paz does not have an air quality monitoring system, so it is difficult to know the quality of the air on the site (SINAICA, 2022), (INEGI, 2019).

Due to the lack of information on the matter, as well as the implications of these data absences, and due to these issues being shared with a lot of other cities around the world, in this study, an a priori-multi tool methodology is proposed based on a spatial correlation approach between on street-level mobile monitoring, factors emissions evaluated and validated by the Environmental Protection Agency (EPA) of the United States of America, a state-of-the-art meteorological modelling system coupled to an air quality model and the application of statistical analysis.

In the present work, the contribution of cruise tourism activities to the air quality in La Paz were analysed in the last days of February in 2018, and the background concentrations of NO_x and SO_x in the area were

estimated as a contribution to furthering our understanding of this complex problem in the context of totally devoid environmental data and to bring light to the importance of multidisciplinary and non-traditional approaches than could lead to a better understanding of pollution patterns and the ways these can be analysed in order to sensitise the public administration to environmental monitoring .

2. Materials and methods

In this study, we divided the methodology into two main approaches: the first was to estimate the impact on air quality based on the estimates of emissions generated by cruise ships using the AERMOD modelling system coupled with WRF; this is described in Sections 2.1 to 2.4 of this paper. The second approach had the objective of estimating the spatial pattern of pollutant concentration in the city at the intersection level in the metropolitan area of La Paz, using low-cost analysers and interpolation processing of the data; this is detailed in Sections 2.5 and 2.6. The final element of the methodology is related to the spatial correlation of the results of these two approaches, and an estimation of the minimal impacts of cruise ship activities at the intersection level was established according to statistical analysis.

2.1. Cruise ship traffic data

The company S&P Market Intelligence (https://www.spglobal.com/marketintelligence/en/mi/industry/maritime.html) was the provider of the database used to identify the traffic of cruise ships in La Paz (arrival, departure, and berthing time) during the whole of 2018. Additional information obtained from the database included: call number, IMO, ship type, movement type, country, name of the ship, port ID, port name, zone name, coordinates, arrival and sail date, hours in port and destination.

2.2. Cruise ship emissions

The traffic cruise data were used to identify the power of each vessel (hp-kW) in order to calculate the emission factor using EPA's Ports Emissions Inventory Guidance: Methodologies for Estimating Port-Related and Good Movement Mobile Sources Emissions (EPA, 2020).

$$tE = P^{*}EF^{*}C^{*}12.9 \quad (1)$$

where tE is the total emission (g/s), P is power of the vessel (kW/h), EF is emission factor of the engine for each navigation and C: conversion factor from hours to seconds (1/3600). We calculated the emissions of cruise ships during hotelling; according to Murena, the value reported was 12.9 % (Murena et al., 2018) of the ship's total power. The three criteria air pollutants used in the present investigation were NO_2 SO_2, and PM_{10}.

2.3. Air dispersion model

Usually, air quality modelling systems (AQMS) require detailed information for the topography, meteorology, and pollutant emissions (González-Rocha et al., 2015). In the following section, these variables are described.

2.3.1. AERMOD

The American Meteorological Society (AMS) and the Environmental Protection Agency (EPA) developed AERMOD, a local air quality model, in 1991 (Kumar et al., 2016). AERMOD is a Gaussian air dispersion model that incorporates building downwash algorithms (Kalhor and Bajoghli, 2017), be executed with real or estimated meteorological information (EPA, 2021b).

The AERMOD model has two important factors related to the estimation of air pollutants: 1) the outputs of the model are 1 h average concentrations (Pandey and Sharan, 2019) and 2) the model is suitable for analysing distances of <50 km from the source (Mokhtar et al., 2014). The software requires meteorological and terrain inputs, which are obtained using a meteorological pre-processor, AERMET, and a terrain pre-processor, AERMAP (Matacchiera et al., 2019).

The meteorological data that the model considers are temperature, dew point, pressure, and solar radiation (O'Shaughnessy and Altmaier, 2011), wind speed, wind direction, total cloud cover and low cloud cover, convective velocity scale, temperature scale, mixing height and surface heat flux (Ma et al., 2013). The AERMET model results are directly introduced into AERMOD (Huang and Guo, 2019).

AERMOD can facilitate coupling with different weather models such as the Weather Research and Forecasting (WRF), the Regional Atmospheric Modelling System (RAMS), the fifth generation of the National Center for Atmospheric Research (NCAR) / the mesoscale model of the Pennsylvania State University (MM5) and Eta Models (Seangkiatiyuth et al., 2011).

2.3.2. Terrain modelling

In order of calculate the concentrations at the receptors positioned at locations with varying elevations, AERMOD simulates a plume as a weighted sum of concentrations from two extreme scenarios: (i) a horizontal plume under very stable conditions and (ii) an elevation-following plume accounting for varying elevations in the area (Zou et al., 2010). In the present work, the best resolution available was the U.S. Geological Survey (USGS) database, while the digital model used was Shuttle Radar Topography Mission (SRTM) with a 30 m resolution. In the case of receptors, a 50 × 50 km mesh with a spacing of 0.5 km was used. A total of 10,201 receptors were used to calculate the airborne pollutants in the area, with the following UTM coordinates as a reference point (Zone 12): 572859.69 m N, 2677783.84 m E (Table 1).

2.3.3. WRF-AERMET

In Mexico, as well as in many other countries, there are regions where it is difficult to install and operate weather stations by which to obtain surface and vertical weather information. Therefore, in order to improve air quality models, it is essential to generate databases, protocols, guides, standards, and indexes able to improve the accuracy of the models and diagnoses that could enhance air quality management (Mendoza-Lara et al., 2021).

Surface and vertical weather data can be obtained from meteorological stations near the study area. However, in the present work, where weather stations are distant, their data may not be representative; this is the reason for using WRF, a cutting-edge mesoscale numerical weather prediction designed both for atmospheric research and operative forecast applications. This model is useful for attaching the weather parameters required for air quality models (Kesarkar et al., 2007).

The WRF system is a multi-agency effort, principally involving the National Center for Atmospheric Research (NCAR), the National Oceanic and Atmospheric Administration (NOAA), the National Centers for Environmental Prediction (NCEP) and the Forecast Systems Laboratory (FSL), the Air Force Weather Agency (AFWA), the Naval Research Laboratory, the University of Oklahoma and the Federal Aviation Administration (FAA) (Afzali et al., 2017).

Table 1
Weather modelling parameters.

Element	Parameter
Forecasting modelling system	WRF
Resolution	4 km
Study area	50 km × 50 km
Time period	1st of January to 31th of December (2018)
Database	GRIB2 ds083.2 NCEP Climate Forecast System Version 2 (National Centers for Environmental Prediction et al., 2000), (Saha et al., 2011)
Reference coordinates	569 957,68 m E, 2 679 310,14 m N, Zone 12

2.4. Technical considerations of the modelling system

As mentioned, cruise ships can be considered to be mobile sources; however, for the present study, only the contribution of emissions during the hotelling stage was estimated; thus, given this condition, the simulation can be considered to be a point source. It is important to mention that AERMOD can model both types of sources: mobile and point sources (Askariyeh et al., 2017) . The source release parameters were considered assuming the following average values: a diameter of 1 m and a gas velocity of 10 m/s (Murena et al., 2018), while the height of the point source was estimated according to the cruise model, namely, between 11 and 17 m in height. To establish the emission times during the hotelling stage, the cruise ship traffic data were considered; within this information, the arrival and sail date were presented. With this data, the emission times of each cruise were determined.

Finally, the EPA emission factors estimate the emission of PM_{10}, SO_2 and NO_x. With respect to the latter pollutant, the model is suitable for considering the physical and chemical characteristics used by the ARM2 method (Kimbrough et al., 2017), which calculates a minimum and maximum NO_2/NO_x ratio. This means that the values presented in the present work only consider the concentration of NO_2 in the air.

2.5. Evaluation

Although there is no methodology for evaluating the sensitivity of meteorological data, we propose the following stages: availability, refining, criteria sufficiency verification and determination of the essential characteristics of the data. For the last stage, the validation of the data demands knowledge about the variables' performance and statistical analysis support.

In the case of the quantitative analysis, the selected analyses were the root-mean-square error (RMSE), the normalised mean absolute error (NMAE), the bias (BIAS), Pearson's correlation coefficient (r) and the adjustment index (IOA). The IOA (index of agreement) contributed to the analysis by providing a general index for the accuracy of the model by comparing it with real data. The matching results are generally classified according to the following scale (Gilchrist, 2009), (Carrisoza Urbina et al., 2015): a) -1 to 0.00, totally inadequate matching, b) 0.01 to 0.39, insufficient consistency, c) 0.40 to 0.75, good concordance, d) 0.76 to 0.99, excellent concordance and e) 1, perfect concordance.

Information from a weather station administrated by the Mexican Meteorological service (abbreviated as SMN according to its Spanish acronym) and the Meteorological Aerodrome Report was used to evaluate the sensitivity of the WRF model (SMN, 2022). The weather station is in the city centre, 4 km away from the reference coordinate of the weather modelling. The variables used in the sensibility analysis were temperature (T), relative humidity (RH), wind speed (WS), wind direction (WD) and atmospheric pressure (AP).

2.6. Georeferenced of pollutant concentration (measurement)

The measurement of pollutants in the study area was obtained using air quality spatial sampling carried out by personnel of the civil association BCSicletos using Arduino-based monitors during 20 and 21 February 2018, dates when no cruise ships were present in the bay. The monitors were designed, built, and calibrated by G.I.M.A. (Interdisciplinary Environmental Monitoring Group of Ensenada) as part of a project of BCSicletos to produce open-access hardware and software for air quality monitoring (Moctezuma Escamilla et al., 2022).

The organization used a methodology based on semi-random routing along the continuous urban area of the city of La Paz to obtain a database of georeferenced points with their corresponding airborne concentrations of criteria pollutants, including PM_{10}, SO_x and NO_x, the criteria pollutants analysed in the present study. The sampling was carried out by bicycle travellers in normal traffic conditions. To avoid atypical sampling derived from irregularities such vehicles passing too close to the sampler or similar issues, the data were spatially smoothed and clustered using 20 m spacing between the centroid points used to create buffers with a 25 % spatial overlap between their covering; this also helped to establish a spatially homogeneous dataset to avoid oversampling in the data and overfitting in the interpolation processes due to the stops on the intersections and the waiting times of traffic lights. The field data were generated using the WGS84 coordinate system, but all the processing and spatial analyses were performed using the ITRF 2008 CCL (EPSG:6372) coordinate system.

The resulting database allowed us to identify the airborne concentrations of the selected criteria pollutants, NO_x and SO_x, that are present in the study area and are produced by different activities and sources, both fixed and mobile.

2.7. Determination of spatial concentration of pollutants using mobile monitoring (interpolations)

The datasets of each day for both pollutants were interpolated using radial basis function (RBF) interpolation with a 500 m range, and a 16-point 4-sector neighbourhood at 35°, with a multi-quadratic kernel function configuration. The results were submitted to a cross-validation process where points, and extreme normalised error values were discarded and then a second RBF interpolation was carried out for each pollutant on each day using the same configuration as that used for the previous RBF interpolation. Finally, the city intersections in the studied area were used to extract the interpolated values of airborne pollutants for each day in order to obtain an almost city-wide dataset that can be used to address ships' influence on the pollutant concentrations.

2.8. Spatial correlation between AERMOD modelling and RBF interpolations

The spatial correlation values were calculated from the AERMOD models and the interpolated values of the pollutants of each day and from pollutants using the differential Moran's I Index with local indicators of spatial association (DiLISA); this was calculated using the following equation:

$$\mu_i = \frac{(x_{i,t} - x_{i,t-1}) * \Sigma_j w_{ij}(x_{j,t} - x_{j,t-1})}{\Sigma_i (x_{i,t} - \underline{x}_{i,t})^2} \quad (2)$$

where w_{ij} is binary weight that indicates neighbourhood adjacency of j samples to i (the intersection in question), j is their neighbouring intersections of i, t is the time or studied event and t-1 = the previous time or base scenario.

In order to properly represent local association, an adjacency weight matrix was created using the same ranges as those used during the RBF interpolation (500-metre threshold); this matrix consisted of binary values (w_{ij}) that force the abovementioned formula to only take into account those neighbouring samples (j) to the one being estimated (i) and omitting every other value from the dataset. The basis of this estimation was a derivative application of the LISA index established by Anselin (Anselin, 1995) and is further explained in (Anselin, 2020).

This estimation was also carried out between days in order to differentiate between the urban zones where day-to-day pollution has an effect, and to determine if they are spatially coincident to the intersections affected by ship pollution. Permutation inferences were used to address the significance of each analysis (999 permutations), followed by clustering based on their place in the Moran's scatterplot and significance, leading to a homogeneous clustering for all the analyses into 5 groups: high-high, low-low, high-low, low-high and non-significant (pseudo $p > 0.05$). This means that each group reflects the differential values of the models and the interpolations and allows us differentiate between low and high constancy and increased or decreased concentrations. For these steps, GeoDa, 1.18.0 software was used.

For the application of this analysis and the results in this paper, it was assumed that the monitoring measurements and interpolations of the concentrations of NO_x and SO_x were equivalent to the concentrations of NO_2 and SO_2, respectively.

2.9. Evaluation of air quality impact and minimum airborne concentrations

Based on the clustering of the data described previously, co-location analyses were carried out to address the spatiotemporal constancy of each pattern of pollutant concentration at the intersection level. The impact of hotelling cruise activities on air quality in the atmospheric basin of La Paz was conducted using airborne concentrations of particulate matter, where particles have an aerodynamic diameter equal to or <10 μm (PM_{10}), sulphur dioxide (SO_2) and nitrogen dioxide (NO_2) established in the Mexican Standar Leves (MSL) (NOM-022-SSA1-2019, 2019; NOM-023-SSA1-2021, 2021) and the World Health Organization's (OMS) Air quality guidelines (AQG), and comparing them to the minimum values observed in the spatiotemporal prevalence of the "no consistency" cluster.

3. Results and discussion

3.1. AERMOD modelling

3.1.1. Meteorology

The WRF modelling and MMIF coupled data generated a single grid cell (4 km) representative of the entire domain. The modelling included an entire year (2018) for each hour and the following variables: sensible heat flux (W/m^2), surface friction velocity (m/s), surface roughness (m) convective velocity (m/s), connective and mechanical planetary boundary layer height (m), Monin–Obukhov length (m), Bowen radius, albedo, surface temperature (K), wind speed (m/s) and direction (°), precipitation (mm), relative humidity (%), surface pressure (mb) and cloud cover. For the meteorology in the vertical direction, the following were obtained: wind speed (m/s) and wind direction (°), surface temperature, standard deviations of wind speed and direction at different altitudes, from 175 to 5000 m above sea level.

The generated surface and vertical meteorology files were input into AERMOD to estimate the dispersion of air pollutant emissions from cruise ships.

As mentioned, five variables were considered to evaluate the sensitivity of the modelling; the results are presented in Table 2.

In general, the wind direction in the study area was predominantly from the south, with almost 23.1 % of the total influenced by Pacific Ocean currents; however, together, wind coming from the north, northeast and northwest represented 46.3 %, whose currents are influenced by the Gulf of California. This is important since the direction of the dispersion clouds emitted by the cruise ships due to hotelling activity can be inferred.

Fig. 1 shows the behaviour of wind direction and Fig. 2 time variation of wind speed. Both figures exhibit comparison between the WRF-AERMET and the measurements of the weather station located in La Paz, for the year 2018.

3.1.2. Dispersion

According to the cruise ship database, there are five different cruises from 1200 hp. to 4520 hp. that arrive at La Paz. During 2018, the ships arrived 41 times with an average berth time of 17.5 h. In accordance with EPA emission factors, the results of the emissions for each type of ship and the maximum impact on air quality in the La Paz air basin are shown in Table 3.

According to the results obtained by the model in relation to particles, it is observed that the impact on air quality is lower compared to NO_2 and SO_2, with an average of 0.19 $\mu g/m^3$ (±0.20). The low impact of PM_{10} is a consequence of several factors, including cruise engine technology, and international regulations regarding the concentration of sulphur in diesel, reducing the emission of SO_2 and Particles.

In this sense, it is important to mention that the particles can have two origins, the primary origin is characterized by being emitted directly from the source, which can be an anthropogenic source (industrial, mobile sources, combustion processes, among others) or natural (dust, sand, spores, marine aerosols, ashes from volcanoes, forest fires, among others). On the other hand, the secondary origin occurs in the atmosphere due to chemical reactions of the precursor gases, for example, SO_x and NO_x, among others.

Taking into account the low concentration levels of PM_{10} obtained in the modelling, it was decided to focus the analysis on the behaviour and concentration of SO_2 and NO_x, in addition to the fact that these atmospheric pollutants are precursors of particles.

Fig. 3A shows the maximum impact on air quality due to SO_2 emissions from the E-type cruise ship identified for the modelling day of December 26, 2018. As shown, although the maximum concentration was found in the body of water, there was a significant contribution found in most of the city of La Paz, highlighting the areas near the port. This means that, for the conditions presented, the predominant wind came from the north. As mentioned, the predominant direction was from the south, but there are currents that derive from the north; this coincides with the behaviour of the atmospheric pollution presented in the image. On the other hand, in Fig. 3B, regarding the behaviour of NO_2 dispersion in the worst scenario identified and generated by the type C cruise the modelling day was detected corresponds to June 16, 2018. The maximum concentration was located near the emission point; however, there was a high influence towards the northeast and southwest.

The maximum concentrations determined by the modelling system are consistent with temporality. For example, the maximum concentration for NO_2 was identified in summer, this pollutant is associated with local emissions and atmospheric chemistry such as ultraviolet radiation, while the maximum concentrations of SO_2 are related to meteorological conditions that do not promote dispersion such as ambient temperature, wind speed and low planetary boundary layer heights, that are generated in winter.

According to the sensitivity evaluation of the meteorological modelling parameters (WRF-AERMET), there was a statistical difference, specifically in the wind direction and wind speed; according to the correlation (r), these variables showed little correlation, 0.14 and 0.17, respectively. However, graphically, the wind speed was found to maintain the same behaviour, with the modelled values being higher as compared those observed. However, as mentioned, the data generated by MMIF for the WRF-AERMET coupling use an average value for the mesh determined for its modelling, which is representative of the data in the study area. In addition, it should be taken into account that the meteorological station where the data were obtained is located far from the coast, so the roughness influences the speed of the coast; therefore, the shear causes the wind speed to decrease. With respect to the wind direction, this variable is cyclic; for this reason, the statistics should be calculated with caution due to the magnitude of the vector correction, given that values between 0 and 360 can be obtained.

Despite this difference, the calculation of the adjustment index (AOI) for these variables, as well as for temperature, relative humidity, and atmospheric pressure, obtained values between 0.40 and 0.68, which indicates that the meteorological modelling system database has a good adjustment index, which translates into an acceptable value allowing the data to be used in the AERMOD model; consequently, the values generated by this model can be considered reliable.

According to the methodology regarding the emission factors generated by the cruise ships, it was identified that they emit between 0.88 and 3.88 g/s during the hotelling stage. In addition, the traffic of this type of vessel during 2018 was considered, which arrived at the port 41 times. For the air quality modelling system, NO_2 and SO_2 dispersion was analysed.

The results showed that the concentrations oscillated depending on the meteorological characteristics of the site. Based on the AERMOD

Table 2
Sensitivity evaluation of the meteorological modelling parameters (WRF-AERMET).

Variable	RMSE	NMAE	BIAS	r	IOA
Temperature	4.13	0.03	−0.87	0.80	0.68
Relative humidity	22.23	0.22	12.06	0.55	0.50
Wind direction	140.01	0.01	0.06	0.27	0.40
Wind speed	2.29	−0.17	−38.8	0.14	0.43
Atm. pressure	2.56	−0.00	−2.40	0.95	0.50

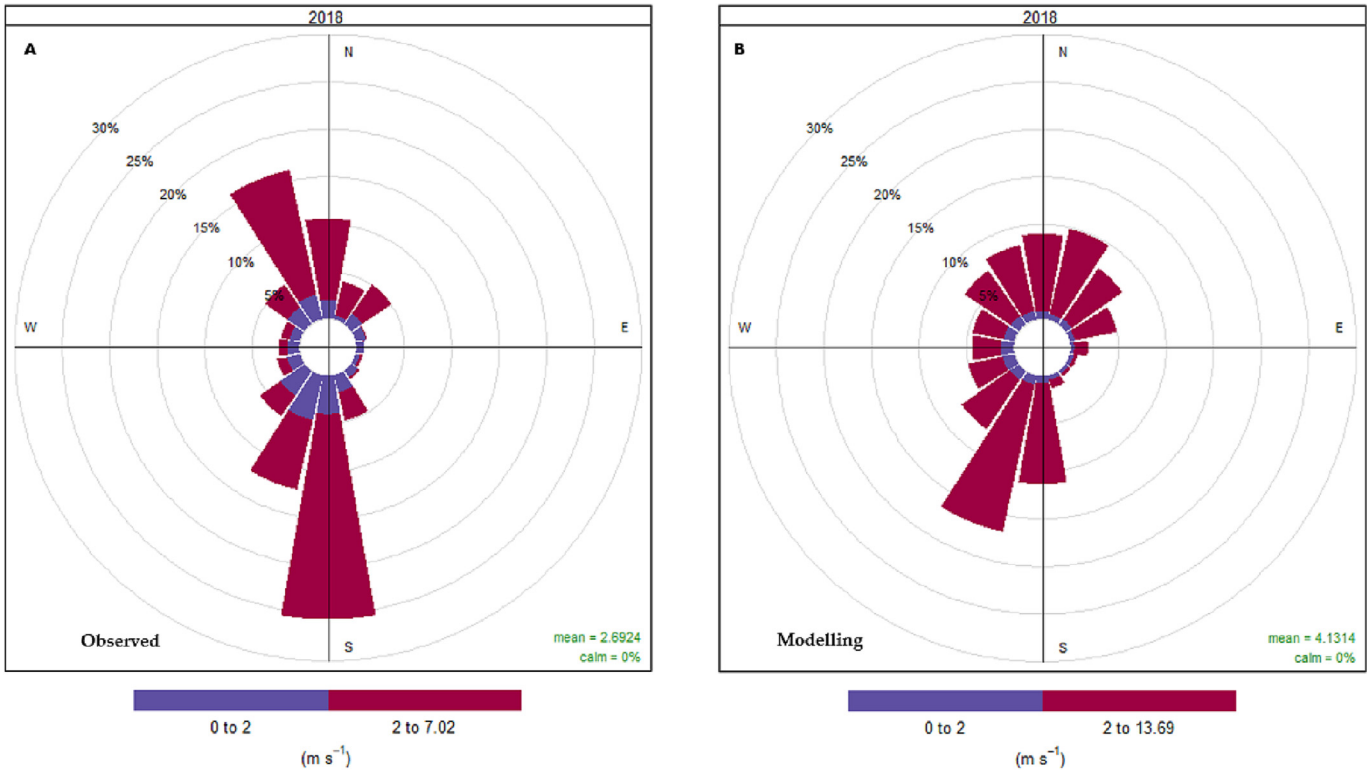

Fig. 1. Comparative wind direction as observed (A) and modelling (B), database to the year 2018.

simulation, it was determined that the air quality impact for NO_2 ranges from 0.72 to 13.66 μg/m^3 with an average of 5.31 μg/m^3 (±3.12), while SO_2 concentrations were found to range from 1.11 to 15.71 μg/m^3 with an average of 5.76 μg/m^3 (±3.57). In the Fig. 3 shows the worst-case atmospheric scenarios for each pollutant.

Taking into account the concentrations of each scenario, it was observed that the maximum concentrations of each air pollutant were close to the emission source. This refers to calm conditions, wind speed and the "building-downwash" effect (Monbureau et al., 2018); therefore, these concentrations do not affect the urban area but do affect the water body, which

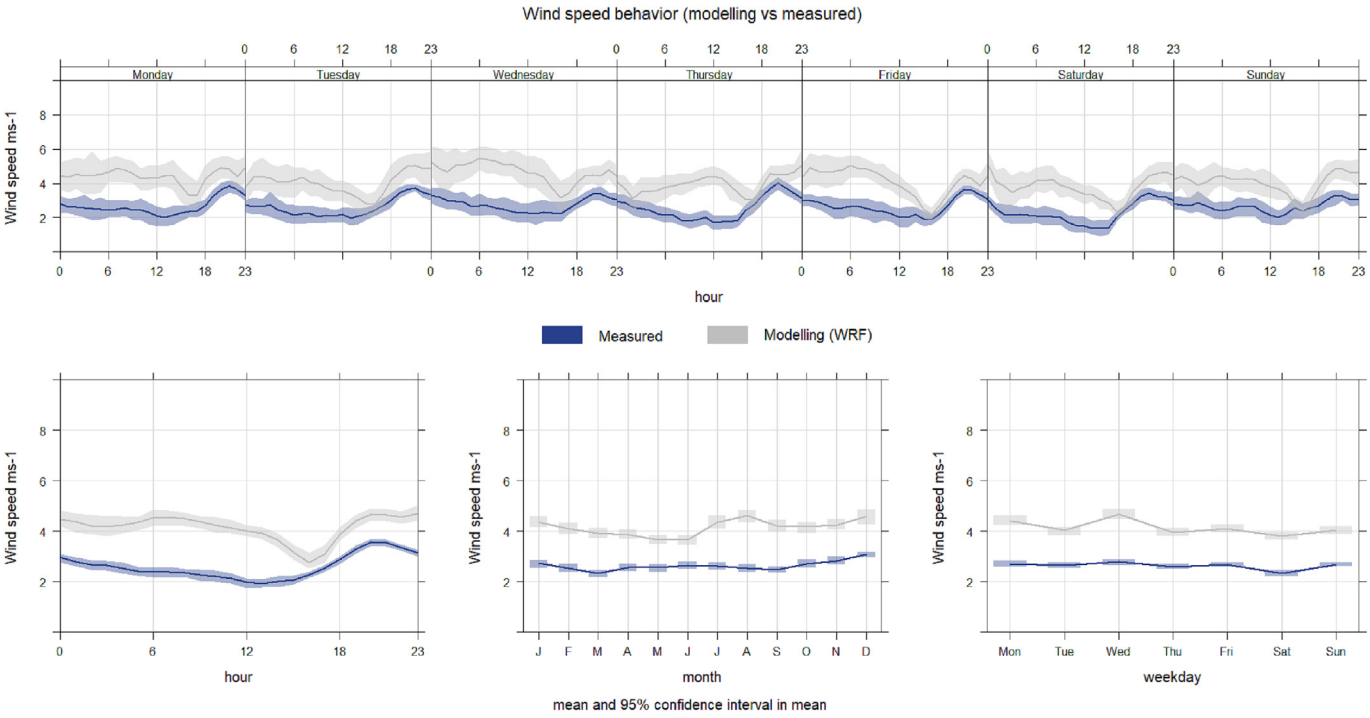

Fig. 2. Comparative wind speed behaviour as observed (blue) and modelling (gray). Time variation average hours per week (A), average hours per day (B), monthly average (C), and daily average per week (D).

Table 3
Emissions for each type of cruise ship and the maximum impact on air quality.

Cruise ship (1)	HP	kW	Fuel	Emissions (g/s)			Maximum impact on air quality (μg/m^3)		
				NOx	SO_2	PM_{10}	NO_2	SO_2(2)	PM_{10}
A	1610	1184.15	Diesel	3.44	2.73	0.07	9.86	10.96	0.39
B	1610	1184.15	Diesel	3.44	2.73	0.07	10.28	11.43	0.49
C	2450	1801.9	Diesel	0.88	4.16	0.02	2.99	15.71	0.06
D	1824	1341.5	Diesel	3.90	3.10	0.08	10.93	9.65	0.42
E	1200	882.9	Diesel	2.47	2.04	0.60	13.66	12.54	1.16
Average							5.31	6.00	0.19
Minimum							0.72	1.11	0.00
Maximum							13.66	15.71	1.16
Standard deviation							3.12	3.68	0.20
Percentage (%) with respect to the MSL							6.83	8.00	1.66
Percentage (%) with respect to AQG (OMS)							6.83	39.28	2.58

1. Model engine: A -1982, B – 1982, C -2018, D – 1983, E – 1994.
2. To standardize the WHO guideline with the Mexican standard, the maximum hourly concentration was considered as a 24-h concentration.

could have a negative impact on the water column, aquatic fauna and submerged aquatic vegetation. Additionally, it was observed that the distribution of air pollution was lower in the urban area of La Paz, with values up to 5 μg/m^3 for SO_2 and up to 3 μg/m^3 for NO_2.

The results of the meteorological modelling using WRF and the AERMOD air quality modelling system for PM_{10}, NO_2 and SO_2 emissions suggest that, due to the operations of the hotelling stage of cruise ships, PM_{10} emissions have a low impact on air quality with an average of 0.19 μg/m^3 (±0.20), NO_2 has an impact on the air quality, with values ranging from 0.72 to 13.66 μg/m^3 with an average of 5.31 μg/m^3 (± 3.12), while the SO_2 concentrations ranged from 1.11 to 15.71 μg/m^3 with an average of 5.76 μg/m^3 (±3.57).

This means that the maximum impact estimated by the model for the atmospheric basin of La Paz due to this activity compared with the Mexican standard levels, represents 1.66 % for PM_{10}, 6.83 % for NO_2 and 7.98 % for SO_2 of the threshold, while he World Health Organization's Air quality guidelines, represents 2.58 % for PM_{10}, 6.83 % for NO_2 and 39.28 % for SO_2 of the threshold.

3.2. Interpolation of air pollutants

Air quality monitoring is a key tool used to determine adherence to air quality norms and to avoid the burden of disease associated with air pollution such as stroke, lung cancer and acute and chronic pneumopathies such as asthma. To effectively assess and evaluate the impact of air pollution in populations and natural resources, it is essential to have systems, networks and air quality monitoring programs (Páramo-Figueroa, 2019) that can provide accurate data and long-term information with transversal compatibility.

The most recent air quality information from the 2021 mobile monitoring stated that the NO_2 Mexican standard levels were exceeded only on five occasions in the year; however, the Mexican standard level of 40 μg/m^3 (annual average) exceeds the WHO's air quality guideline values of 10 μg/m^3 (annual average) (WHO, 2022) by four times, resulting in a complex regulatory problem that can only be solved by proving the need to lower the criteria levels stated in the law, with statistical and spatial analyses being a key element in achieving this goal.

In Mexico, there is a gap regarding the compliance with laws related to air quality. It is mandatory that cities with up to 150,000 inhabitants must have an air quality monitoring system in operation; however, only 44 to the total 98 cities fulfil this requirement (SINAICA, 2022). According to its responsibilities, the Mexican Air Quality Information System has operative problems reflected in the fact that up to 58 % of cities do not have enough information to assess compliance with official standards. This is an issue even when the standards are known, and cities try to comply due to the lack of proper reference data generation mechanisms. On the other hand, only 19 %, 4.5 % and 7 % of the results obtained by the functional stations complied with the ozone, PM_{10} and $PM_{2.5}$ standards, respectively (SEMARNAT, 2020), showing a clear pattern where most cities either cannot comply or lack the means to do so.

In the case of La Paz, there is no monitoring station for pollutants, only a weather station than provides basic data. This drives non-governmental organisations to design and operate means by which to create the datasets for mobile air quality monitoring in order to obtain information by which to identify the level of the city's adherence to air quality standards.

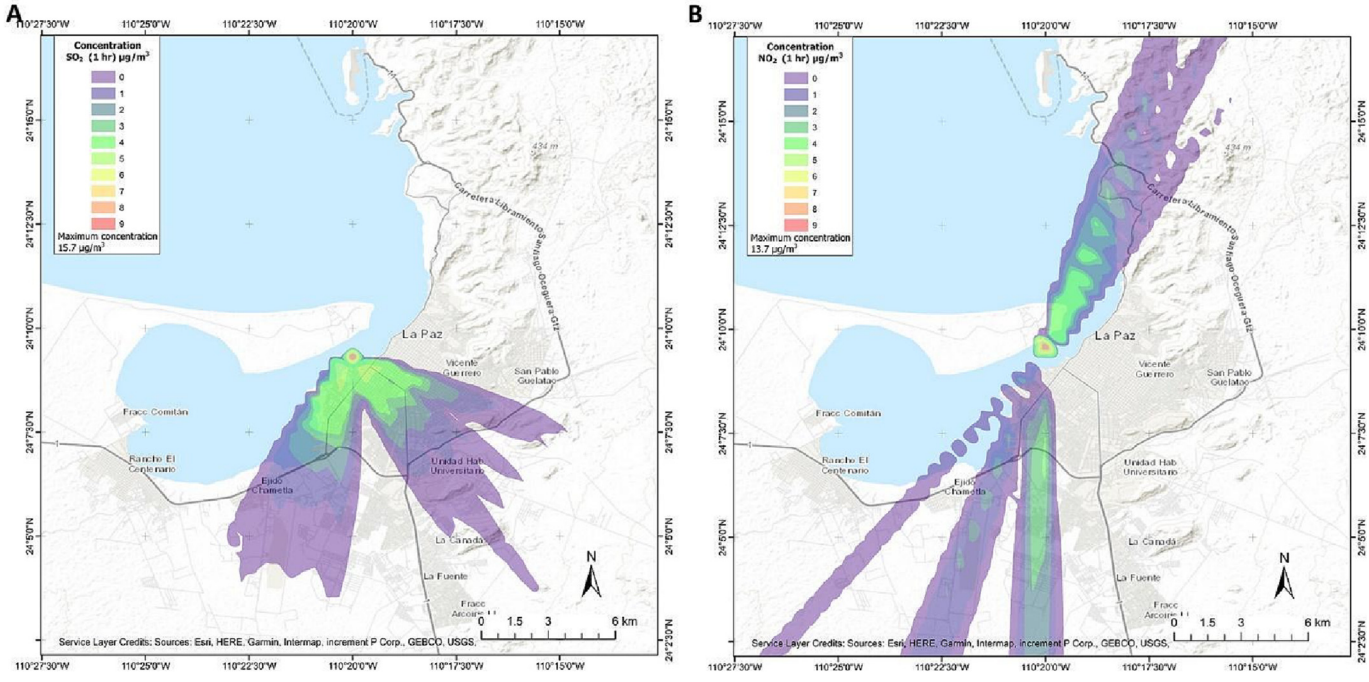

Fig. 3. Worst-case atmospheric scenarios for each pollutant. (A) Dispersion plume of SO_2 for an E-type cruise ship modelling for December 26, 2018. (B) Dispersion plume of NO_2 for a C-type cruise ship modelling for June 16, 2018.

Regarding the measurement of air quality, the methodology applied to estimate airborne concentrations in the La Paz Bay using street-level data resulted in values of 0.03 μg/m^3 for SO_x and 8.78 μg/m^3 for NO_x.

3.2.1. Precision of SO_x interpolations

The interpolations conducted for February 20 and 21 showed a trend of pollutant accumulation that increased during the second day of sampling. The means of both datasets (0.148 and 1.17 μg/m^3, respectively) and their ranges exhibited consistency during the interpolation process that allowed us to accurately estimate the level of pollutants in the city through the samplings carried out.

As shown in Fig. 4A, the subsampling process of the original data of 20 February emphasises the variable concentrations between 0.1 and 0.2 μg/m^3 and 0.3 and 0.45 μg/m^3, while a density decrease was identified between 0.2 and 0.3 μg/m^3. Cross-validation confirmed a 3.8×10^{-5} mean calculated error between the subsampling and the first interpolation and 3.7×10^{-5} between the first and second interpolation, which was where the intersection values were set.

A comparison of the original sampling and the intersection dataset (Fig. 4A) showed a considerable adjustment, especially in the 0.08 and 0.3 μg/m^3 range. Values below 0.08 μg/m^3 exhibited a high number of intersections located far away from the port, while intersections above 0.48 μg/m^3 showed a frequency reduction. This latter behaviour can be understood as a way to discard atypical and isolated values, phenomena clearly observable in the media subsample adjustment that estimated the mean (0.11 μg/m^3) below the initial value but with the benefit of urban scale estimation.

The data from 21 February showed a similar behaviour tendency in the analysed process (Fig. 4B); the original dataset showed a mean of 0.17 μg/m^3, while the intersection's mean of the variable was 0.13 μg/m^3.

Both the subsample data and the interpolation values were closer to those of the original sampling. The calculated mean error was 8.7 × 10–5 between the subsample and the first interpolation and had a slightly high value of 10.9×10^{-5} between interpolations. At the intersection level, the number of values between 0.03 and 0.12 μg/m^3 were increased, again as a result of the distance from the port.

3.2.2. Precision of NOx interpolations

The NO_x airborne concentrations exhibited better stability during the interpolation process (Fig. 4C) as compared with those obtained for SO_x pollutants. The 20 February datasets maintained a close mean value between each step with 21.77 μg/m^3 for the field sampling, 21.15 μg/m^3 for the subsampling dataset, 20.47 μg/m^3 for the first cross-validation and 19.41 μg/m^3 for the intersection dataset; the mean errors for each interpolation were -7.66×10^{-3} and -2.42×10^{-2}, respectively.

Values above 24 μg/m^3 (third quartile) were very similar but with lowered frequencies in each step of the process, while the frequencies pattern maintained the same ranges. The inclusion of peripheral intersections

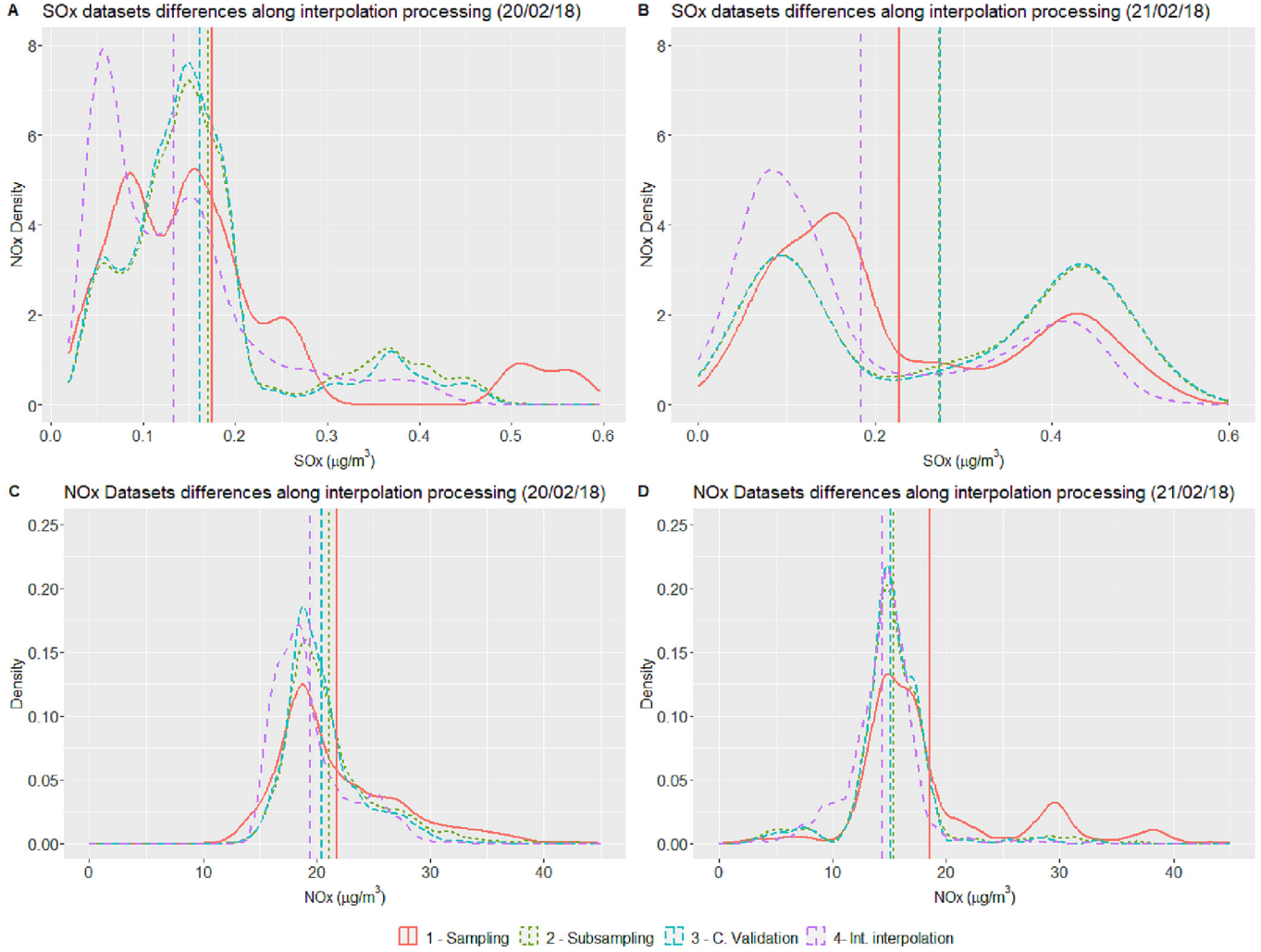

Fig. 4. Dataset composition differences during the interpolation processing steps for SO_x and NO_x concentration on 20 February 2018 and 21 February 2018. Density lines represent smoothed data. Density values refer to the relative frequency of intersections for data of the same dataset (n/N) in relation to the concentration bin ranges of the same pollutant.

for the interpolation samplings barely influenced the mean and median values of all the datasets, even when there were considerable high NO_x concentration data in the sampling dataset. This behaviour was expected and was a main element for selecting the RBF interpolation method over others used for airborne pollutants, such as the Kriging, Voronoi or IDW methods (Bezyk et al., 2021).

In the 21 February datasets, some higher-concentration data points were present in the field sampling, possibly due to local sources such as speeding vehicles or small fixed sources; nevertheless, these concentrations almost disappeared during processing and the pattern remained the same with mean values of 18.57 (1), 15.4 (2), 15.12 (3) and 15.93 μg/m^3 (4) for the respective datasets (Fig. 4D). The mean errors for the interpolations were -1.70 × 10^{-3} and -1.19 × 10^{-2} for steps 3 and 4, respectively.

The methodology followed in this work allowed us to precisely identify the level of pollutants in the different areas that conforms to the city based on near-ground pollutant monitoring (Moctezuma Escamilla et al., 2022).

According to (Bezyk et al., 2021), the optimisation of the air quality monitoring network for carbon dioxide in a medium-large city is a significant issue and requires advanced interpolation processing and modelling methods to handle time series with large gaps in measurements; this methods need to be precise, and needs to consider the spatial distribution of the sampling data points and establish a proper spatial distribution for interpolated value recollection in order to generate an accurate dataset that completely reflects the phenomena while surpassing hyper-local spikes in concentrations and foul data that could cause errors in the interpolation process, especially for extract interpolation methods.

3.3. Spatial correlation between the AERMOD model and RBF interpolation at the intersection level

The results of the simulation of airborne cruise ship pollutants identified a specific area of 1.03 ha (NO_x) and 3.60 ha (SO_x) located west of La Paz city. In this area, the pollutants related to cruise ships were found to contribute up to 5 μg/m^3 of SO_x and up to 3 μg/m^3 of NOx. The identification of the coastal areas impacted by cruise shipping pollution is the first step in scientifically identifying sources of pollution so as to effectively assess air quality policies and programs.

One way to address this issue is by comparing the modelled values and field data to provide insights on how the port contributes and changes the concentrations of the pollutants in the city, and, more importantly, how these values can explain the spatial correlation of the sources that generate them and their dispersion in the city.

Spatial correlations not only shed light on how pollutants behave spatially but also on what influences their concentrations. Other approaches have used these methods to identify sources of pollution (Qi et al., 2022) from transmission channel, and even to link pollutant concentrations to mobile sources, such as traffic, and specific parts of the road network (Reche et al., 2022), showing the great flexibility of the spatial data analysed, and the results that can be obtained from such data.

3.3.1. SOx pollutants

Interpolated SO_x pollutant concentrations at the intersection level presented a clear spatially clustered pattern for both lower and upper concentrations related to the AERMOD model coverage; values of 0.16 μg/m^3 and higher formed corridors either inside the model or in the north part of the city and parallel to the coastline (Fig. 5).

The airborne concentrations for 21 February showed higher concentrations than those seen the previous day, but most of the lower ones remained in the same positions, mostly towards the eastern side of the urban area. Some of these intersections share a spatial location with a corridor that connects the coastal zone of the city with the two urban ways in the city that have a greater traffic demand, namely, Forjadores Blvd. and General Agustin Oalachela Blvd. intersection with 5th of February Avenue.

One of the main differences between the 20 February (Fig. 5A) and 21 February (Fig. 5B) scenarios was that, of the 587 of intersections outside the AERMOD coverage (31.56 % of the total considered), only 39.53 % were above their mean value on 20 February, but on 21 February, 51.78 % were over the dataset mean, showing and increase in pollutants outside the model.

The elevation patterns showed mild-to-low negative correlations to airborne SO_x concentrations as data alone (20 Feb Pearson: −0.53, $p < 2.2e\text{-}16$; 21 Feb: −0.30, $p < 2.2e\text{-}16$) and as spatial patterns (20 Feb Moran's I: −0.53, $p < 0.05$; 21 Feb Moran's I: −0.29, $p < 0.05$); only 29.13 % of all the intersections' elevation was above 35 m above sea level, and, of those,

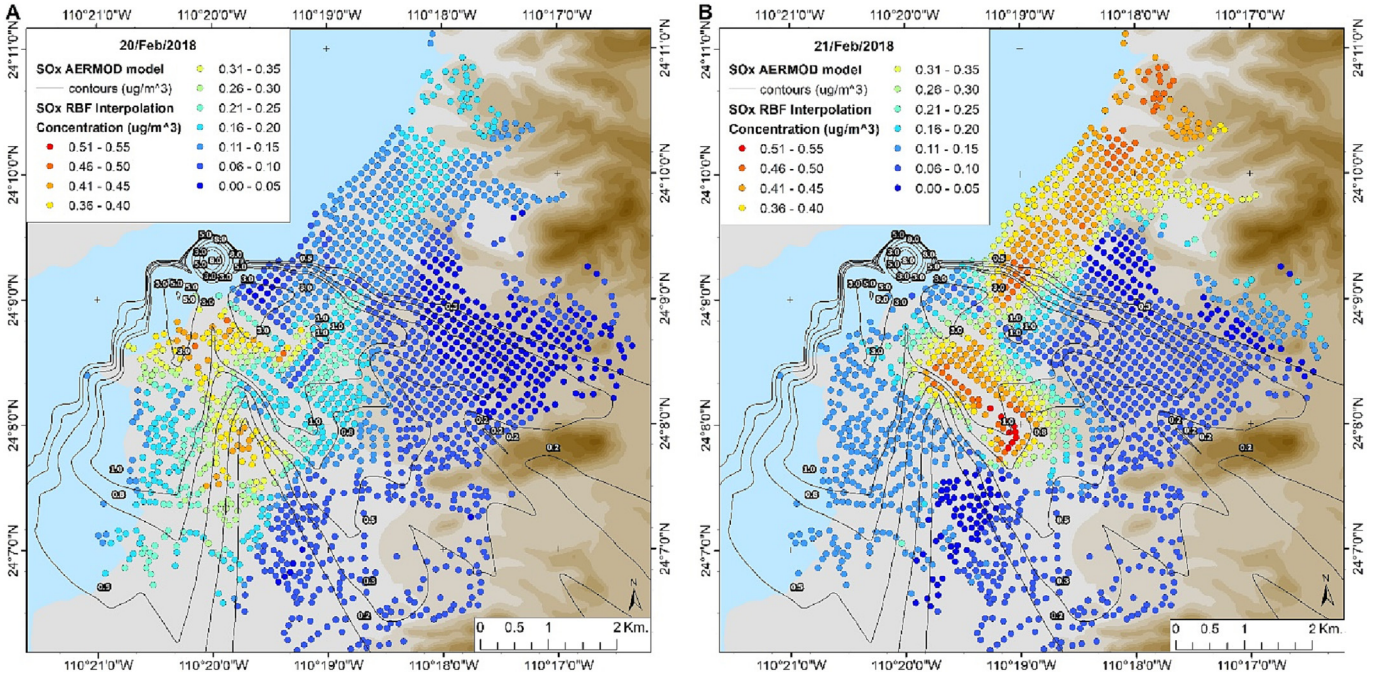

Fig. 5. Spatial comparison between the AERMOD model and RBF interpolation samplings at the intersection level for SO_x pollutants. (A) 20 February scenario comparison. (B) 21 February scenario comparison.

89.19 % and 77.54 % had values under 0.10 μg/m^3 for each day, which were half of the minimal and most common AERMOD model value estimations.

The DiLISA analysis presented a more detailed spatiotemporal scenario showing high levels of spatial clustering between the SO_x concentration differences (Moran's $I = 0.95, p \geq 0.05$). Two clearly distinguishable and significant clusters were formed, both spatially wide and both with different spatial arrays: one with high differential rates and one with low ones; both presented some sparse and unconnected pockets and were delimited by non-statistically significant correlations. Both of them were completely bounded in the AERMOD dispersion model coverage; only the low cluster had more intersections inside (77.88 %) as compared to the high-difference cluster (32.07 %).

No high-low or low-high differential correlation clusters were formed either in this comparison or in the following ones for this pollutant, and only 65.65 % of all the intersections spatially matched the AERMOD model coverage, but, even when the model covered more than half of the intersections, 66.22 % of them lacked statistical significance in the spatial correlation analysis.

When estimating the DiLISA index using each day's RBF interpolated values as the pollutant baseline and the AERMOD values as the "event", high spatial clustering of differences was also observed on both days; concentrations of 1.0 μg/m^3 showed a clear influence as the main delimiter of high pollution related to ships' activity. On 20 February, a Moran's I index of 0.89 was estimated ($p \geq 0.05$), showing a high clustering spatial pattern; a 241-intersection cluster showed a high influence of ships' pollutants with SOx concentration differences ranging between 0.54 and 2.95 μg/m^3 (mean = 1.12, S.D. = 0.71).

In the low-influence cluster, the differential values showed SO_x concentrations above the AERMOD model estimations, with 593 intersections clustered in two groups of low influence of ships' pollutants, one cluster covering almost all the northeast of the city (444 intersections, mean = −0.11, S.D. = 0.04) and one cluster between the two main corridors of the AERMOD model (149 intersections, mean = −0.13, S.D. 0.11), meaning that these concentrations are related to sources other than cruise ships that dock or arrive at La Paz port.

3.3.2. NO_x pollutants

The pollution patterns related to NO_x were significantly different from those that SO_x showed in at least three main aspects: First, the coverage of the AERMOD dispersion showed a considerable concentration difference towards the interpolated values (Fig. 6A and B); second, the AERMOD intersection's coverage had only a few sampling data, with coverage of 7.71 % on 20 February and 1.96 % on 21 February, affecting the interpolation dataset's coverage (5.99 % and 4.37 %, respectively), and even when the RBF interpolation sampling had more spatial coverage at the intersection level (13.86 %), the spatial coverage was still narrow for the correlation analysis.

Elevation was found to be weakly correlated with NO_x concentrations (20 Feb: Pearson: −0.19, $p < 4.84e^{-15}$; 21 Feb: −0.31, $p < 2.2e^{-16}$) even at the spatial level (20 Feb: Moran's I: −0.18, $p < 0.05$; 21 Feb: Moran's I: −0.31, $p < 0.05$); but overall, they remained low in pollutant concentrations, with only 18.00 % of the 472 intersections having above-mean levels on 20 February and 11.22 % of them being above average on 21 February.

The analysis also showed a decreasing tendency of the pollutant over time, implying than even when there is some accumulation of the pollutant in certain higher areas, most of them have a lower presence of NO_x as the elevation becomes higher. Urban intersections that have higher concentrations tended to be closer to the port and in the north part of the city, while those with lower concentrations were present in the south on 20 February and across all of the city on 21 February, and even in a large part of the AERMOD coverage area.

The differential values showed little to no impact at all from the AERMOD model concentrations in relation to the full NO_x sampled values. No intersections had a dominant input from the model, and the Moran's I value for both days were the same for the differential analysis and autocorrelation estimates (0.91 and 0.89, respectively), showing that the NO_x concentrations present in the urban area are not related to cruise activities but to other sources that this study has not covered due to methodological constraints; further analysis will be presented in further publications.

3.4. Clustering co-location analysis and airborne concentration estimation

As differential clustering sheds light on the spatial patterns shown for each pollutant, temporal comparisons can be also addressed in a quite precise way and expressed in cluster consistency among days, even when the mean values of each dataset are different; this is because of the nature of

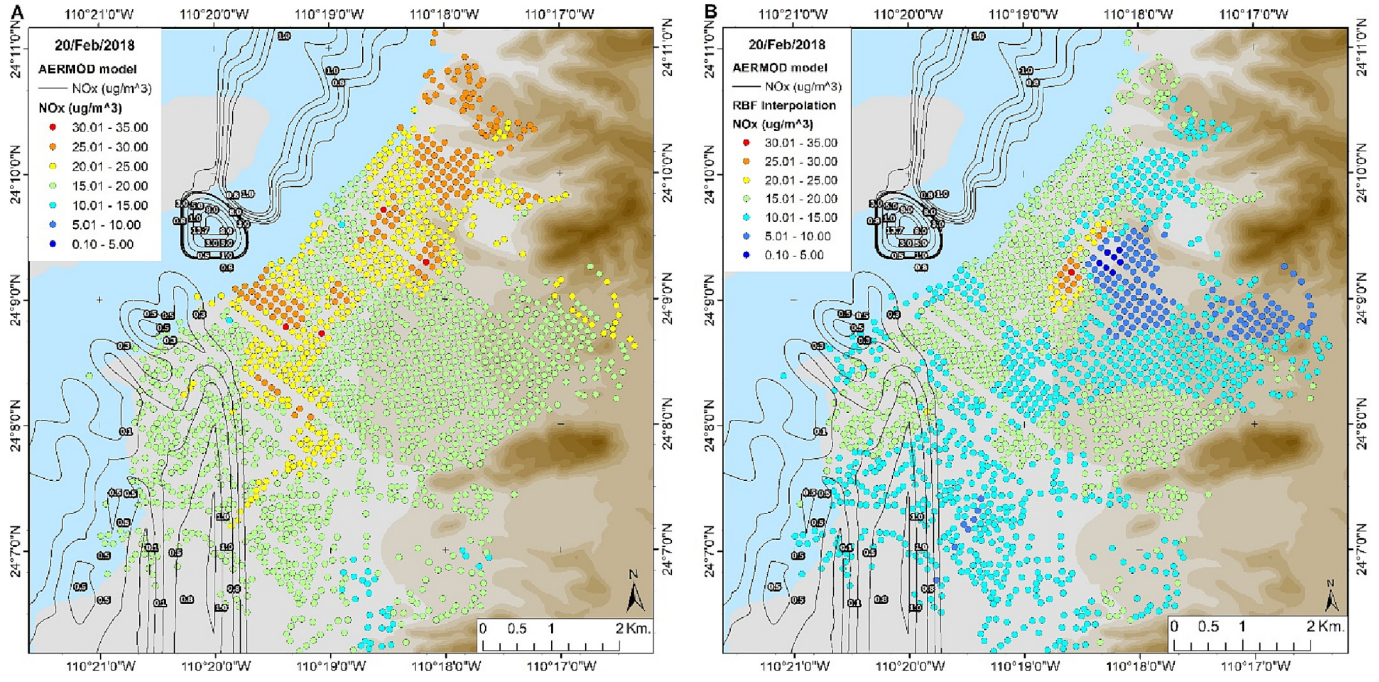

Fig. 6. Spatial comparison between the AERMOD model and RBF interpolation samplings at the intersection level for NO_x pollutants. (A) 20 February scenario comparison. (B) 21 February scenario comparison.

Moran's I clustering, which groups values according to their above- or below-mean position.

For SO_X, the low-low cluster was completely outside the AERMOD model coverage, while the high-high cluster was almost completely inside the area with contributions of >1.0 μg/m^3 from the cruises; no significance cluster was sparse inside or outside the model coverage, but mostly outside. The characteristics of each cluster can be seen in more detail in Fig. 7.

The SO_x scenarios showed a clear difference in the minimal values of those intersections influenced by cruise activities in La Paz port and those that were not influenced by cruise activities, with values of 0.05 ± 0.01 μg/m^3 when the intersections were influenced by cruise activity and 0.03 ± 0.01 μg/m^3 for those whose SO_x pollution was not related to the port. Wider variation was found for those intersections that did not present cluster constancy with minimal values of 0.02 ± 0.02 μg/m^3, a mean value of 0.19 ± 0.034 μg/m^3 and DiLISA values either near 0.75 or 0.00 (Fig. 7D and E).

The co-location analysis of the DiLISA index for SO_x also allowed us to identify an area located in the east of La Paz where the cruise ship contribution to the airborne concentration of La Paz was directly over the sea. In this area, the airborne concentration of SO_x calculated by the AERMOD model (red) exceeded the airborne concentration of this pollutant by up to 2.96 μg/m^3, a concentration that could threaten the mangroves and wildlife on the coast, as well as waterbodies and the population residing near this area. Intersections with high levels of SO_x in the mobile monitoring (blue) were found to be related to sources of pollutants inside the city other than those from cruise ships. A further analysis for the identification of the origin and dispersion of SO_x is needed. The preliminary sources identified the cargo ships of Pichilingue port and the two energy plants. The monitoring of these pollutant sources is necessary to more thoroughly identify their emissions throughout the day and their dispersion patterns.

The NO_x scenarios, on the other hand, showed a lack of influence from the cruise activities, even to the point that almost all the intersections inside the AERMOD model coverage belonged to the cluster lacking statistical significance (Fig. 8C), showing a near-0.00 DiLISA index and the clear observation of a random spatial distribution, especially on 21 February in comparison to the previous day (Fig. 8D). The minimal values of the "no consistency" cluster were the only ones that have importance for this pollutant, with a concentration of 8.78 ± 5.99 μg/m^3 of NO_x and a mean value of 16.84 ± 2.70 μg/m^3. The estimated values for the high-high cluster were almost equivalent (minimum: 12.57 ± 3.54, mean: 14.08 ± 2.78) in range, and thus, do not bring new information to the port pollution analysis, nevertheless, further analysis could be done in order to better understand urban pollution patterns for this particular pollutant.

Most of the intersections showed variance in clustering consistency or no statistical significance (Fig. 8D), indicating that the spatial relationships of airborne pollutants require more variables (and sources) included in such studies, possibly from mobile sources, in order to provide significant results.

4. Conclusions

This study proposes a novel methodology to join databases of field survey data (using low-cost analyzers) and the resulting estimates of air pollutant concentrations with the calculated values of the AERMOD modelling system coupled with WRF generated by cruise ships emissions. The results of the spatial pattern of pollutant concentration based on the use of differential Moran's I Index with local indicators of spatial association (DiLISA) can determine pollution at the intersection level with enough confidence to be of use for urban places where formal pollution surveys are not implemented.

The results highlight the importance of effective air quality management and monitoring in La Paz, Baja California, considering the expansion plans for cruise ship activity in the study area. The authors consider that the proposed methodology and its results bring new insights to pollution source identification in La Paz city and could be of great use for other locations where air quality monitoring data are not being generated or are not openly accessible to the population. On the other hand, further research may analyse the impact of cargo ships and power plants on the air quality of La Paz's Bay.

CRediT authorship contribution statement

Conceptualization, A.I.P.H. and A.O.L.P.; methodology, O.O.M.L., A.O.L.P. and J.M.B.R.; software, O.O.M.L. and A.O.L.P.; validation,

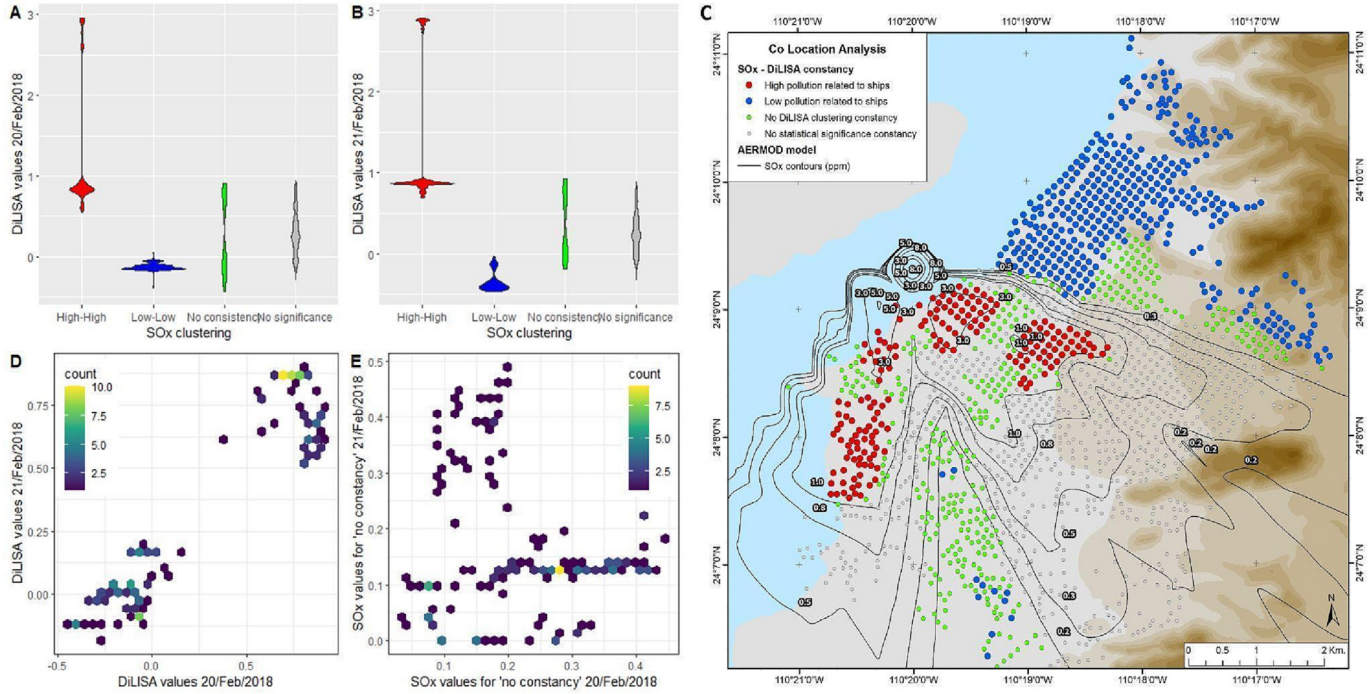

Fig. 7. Co-location analysis of differential DiLISA spatial correlations for SO_x pollutants. (A) Clustering for 20 Feb. (B) Clustering for 20 Feb. (C) Map of spatial distribution of clusters with SO_x pollution related to cruise ships from La Paz port. (D) DiLISA values for "no consistency" cluster. (E) SO_x concentrations (μg/m^3) for "no consistency" cluster. Colours in graphs A and B correspond to colours in map C.

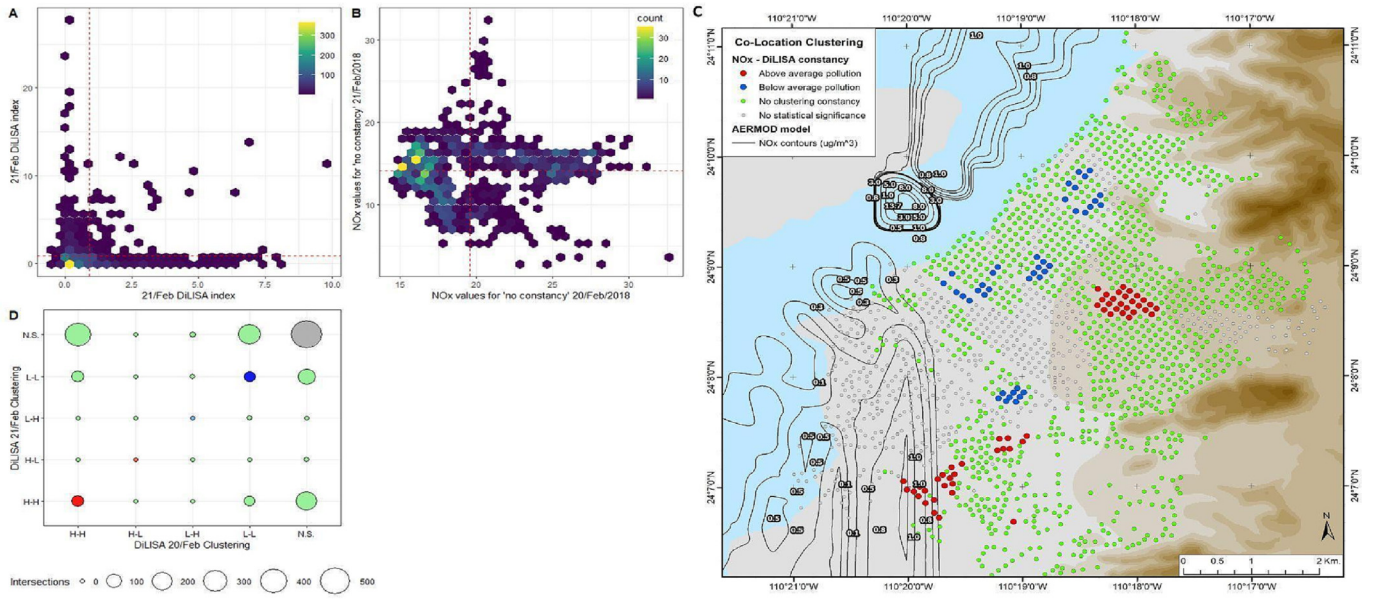

Fig. 8. Co-location analysis of differential DiLISA spatial correlations for NO_x pollutants. (A) Comparison of DiLISA values between days. (B) NO_x concentration comparison for "no consistency cluster" between days. (C) Map of spatial distribution of clusters with NO_x pollution related to itself. (D) DiLISA intersection clustering disaggregation. Colours in graph D correspond to those in map C.

A.I.P.H. and J.M.B.R.; formal analysis, J.M.B.R.; investigation, C.Y.O.M. and A.I.P.H.; resources, A.I.P.H. and C.Y.O.M.; data curation, O.O.M.L; writing—original draft preparation, O.O.M.L., A.O.L.P., A.I.P.H., and C.Y.O.M.; writing—review and editing, A.O.L.P. and A.I.P.H.; visualization, A.O.L.P.; supervision, J.M.B.R., A.O.L.P. and C.Y.O.M.; project administration, O.O.M.L. and A.I.P.H.; funding acquisition, A.I.P.H. and C.Y.O.M. All the authors have read and agreed to the published version of the manuscript.

Funding

This research received no external funding.

Data availability

The authors do not have permission to share data.

Declaration of competing interest

The authors declare that they have no known competing financial interests or personal relationships that could have appeared to influence the work reported in this paper.

Acknowledgments

We extend special thanks to BCSicletos, Colectivo de ciclismo urbano, A.C., for providing the street-level sampling data used in this research paper; to Maria Elena Barrios and IHS Markit for providing databases about ships' activity in La Paz and Pichilingue ports; and to the National meteorological service (Servicio Meteorológico Nacional) for the climate data required for the modelling process.

References

Afzali, A., Rashid, M., Afzali, M., Younesi, V., 2017. Prediction of air pollutants concentrations from multiple sources using AERMOD coupled with WRF prognostic model. Journal of Cleaner Production. Vol. v. Elsevier Ltd., p. 166 Issue 3.

Anastasopolos, A.T., Sofowote, U.M., Hopke, P.K., Rouleau, M., Shin, T., Dheri, A., Peng, H., Kulka, R., Gibson, M.D., Farah, P.-M., Sundar, N., 2021. Air quality in Canadian port cities after regulation of low-Sulphur marine fuel in the North American Emissions Control Area. Sci. Total Environ. 791, 147949. https://doi.org/10.1016/j.scitotenv.2021.147949.

Anselin, L., 1995. Local indicators of spatial association—LISA. Geogr. Anal. 27 (2), 93–115. https://doi.org/10.1111/j.1538-4632.1995.tb00338.x.

Anselin, L., 2020. "Differential Local Moran". Local Spatial Autocorrelation (2). Other local spatiual autocorrelations statistics. Geodacenter. https://geodacenter.github.io/workbook/6b_local_adv/lab6b.html#differential-local-moran.

Askariyeh, M.H., Kota, S.H., Vallamsundar, S., Zietsman, J., Ying, Q., 2017. AERMOD for near-road pollutant dispersion: evaluation of model performance with different emission source representations and low wind options. Transp. Res. Part D: Transp. Environ. 57, 392–402. https://doi.org/10.1016/j.trd.2017.10.008.

Bezyk, Y., Sówka, I., Górka, M., Blachowski, J., 2021. GIS-based approach to spatio-temporal interpolation of atmospheric CO2 concentrations in limited monitoring dataset. Atmosphere. Vol. 12. https://doi.org/10.3390/atmos12030384.

Carrisoza Urbina, J., Flores Velázquez, E., Gutiérrez Reyes, J.A., Juárez López, N.O., 2015. Wettbewerb Berufliche Schulen Dokumentation des Wettbewerbs ... mit den Preisträgerinnen und Preisträgern. Veterinaria México OA. Vol. 2. Landesstiftung Issue 3.

Chatzinikolaou, S.D., Oikonomou, S.D., Ventikos, N.P., 2015. Health externalities of ship air pollution at port – Piraeus port case study. Transp. Res. Part D: Transp. Environ. 40, 155–165. https://doi.org/10.1016/j.trd.2015.08.010.

Chen, T.-M., Kuschner, W.G., Gokhale, J., Shofer, S., 2007. Outdoor air pollution: nitrogen dioxide, sulfur dioxide, and carbon monoxide health effects. Am. J. Med. Sci. 333 (4), 249–256. https://doi.org/10.1097/MAJ.0b013e31803b900f.

CLIA, 2020a. 2020 State of the Cruise Industry Outlook.

CLIA, 2020b. Economic Impact. Economic Impact Fact Sheet. https://cruising.org/-/media/Facts-and-Resources/CLIA_Economic-Impact-Factsheet_June-2020_Global#:~:text=Global-cruise-operations-greatly-benefit,billion-in-salaries-and-wages.

CLIA, 2022. 2022 State of the Cruise Industry Outlook.

Corbett, J.J., Winebrake, J.J., Green, E.H., Kasibhatla, P., Eyring, V., Lauer, A., 2007. Mortality from ship emissions: a global assessment. Environ.Sci.Technol. 41 (24), 8512–8518. https://doi.org/10.1021/es071686z.

Cruise Market Watch, 2022. 2021 worldwide cruise line market share. Market Share. https://cruisemarketwatch.com/market-share/.

EPA, 2020. Port Emissions Inventory Guidance: Methodologies for Estimating Port-related And Goods Movement Mobile Source Emissions EPA-420-B-20-046, September 2020.

EPA, 2021a. Health and environmental effects of particulate matter (PM). Particulate matter (PM) pollution. https://www.epa.gov/pm-pollution/health-and-environmental-effects-particulate-matter-pm.

EPA, 2021b. User's Guide for the AMS/EPA Regulatory Model e AERMOD. EPA 454/B 03 001.

EPA, 2021c. Volatile organic compounds' impact on indoor air quality. Indoor air quality (IAQ). https://www.epa.gov/indoor-air-quality-iaq/volatile-organic-compounds-impact-indoor-air-quality.

Fuentes García, G., Baldasano Recio, J.M., Sosa Echeverría, R., Granados Hernández, E., Zamora Vargas, E., Antonio Duran, R., Kahl, J.W., 2021a. Estimation of atmospheric emissions from maritime activity in the Veracruz port, Mexico. J. Air Waste Manag. Assoc. 71 (8), 934–948. https://doi.org/10.1080/10962247.2021.1902421 Issue 3.

Fuentes Garcia, G., Sosa Echeverria, R., Baldasano Recio, J.M., W. Kahl, J.D., Granados Hernandez, E., Alarcon Jimenez, A.L., Antonio Duran, R.E., 2021b. Atmospheric Emissions in Ports Due to Maritime Traffic in Mexico. J. Mar. Sci. Eng. 9 (11), 1186. https://doi.org/10.3390/jmse9111186.

Garduño, M., 2021. Pese a parálisis de 15 meses, cruceros explorarán estas 4 rutas nuevas en México. July 15Forbes Mexico.

Gilchrist, J.M., 2009. Weighted 2 x 2 kappa coefficients: recommended indices of diagnostic accuracy for evidence-based practice. J. Clin. Epidemiol. 62 (10), 1045–1053. https://doi.org/10.1016/j.jclinepi.2008.11.012.

González-Rocha, S.N., Mendoza-Lara, O.O., Fuentes-Gea, V., Baldasano, J.M., 2015. Assessment of meteorological models for air pollution transport: analysis between Mexico and Puebla metropolitan areas. A: 3rd BSC International Doctoral Symposium. Book of abstracts. Barcelona Supercomputing Center, pp. 46–48.

Huang, D., Guo, H., 2019. Dispersion modeling of odour, gases, and respirable dust using AERMOD for poultry and dairy barns in the Canadian prairies. Sci. Total Environ. 690, 620–628. https://doi.org/10.1016/j.scitotenv.2019.07.010.

IMO, 2020. IMO 2020 cutting sulphur oxide emissions. https://www.imo.org/en/MediaCentre/HotTopics/Pages/Sulphur-2020.aspx.

INEGI, 2018. Programa de Gestión para Mejorar la Calidad del Aire del estado de Baja California Sur (2018-2027).

INEGI, 2019. Información Nacional de la Calidad del Aire 2019. https://cambioclimatico.gob.mx/informe-nacional-de-calidad-del-aire-2019-mexico/.

Islas-Rivera, V.M., Moctezuma-Navarro, E., Hernández-García, S., Lelis-Zaragoza, M., Ruvalcaba-Martínez, J.I., 2011. Urbanización y motorización en México.

Kalhor, M., Bajoghli, M., 2017. Comparison of AERMOD, ADMS and ISC3 for incomplete upper air meteorological data (case study: steel plant). Atmos.Pollut.Res. 8 (6), 1203–1208. https://doi.org/10.1016/j.apr.2017.06.001.

Kalosh, A., 2021. Major cruise developments coming to Mexico's Ensenada and La Paz. Seatrade Cruise News. https://www.seatrade-cruise.com/ports-destinations/major-cruise-developments-coming-mexicos-ensenada-and-la-paz.

Kesarkar, A.P., Dalvi, M., Kaginalkar, A., Ojha, A., 2007. Coupling of the weather research and forecasting model with AERMOD for pollutant dispersion modeling. A case study for PM10 dispersion over Pune, India. Atmos. Environ. 41 (9), 1976–1988. https://doi.org/10.1016/j.atmosenv.2006.10.042.

Kimbrough, S., Chris Owen, R., Snyder, M., Richmond-Bryant, J., 2017. NO to NO2 conversion rate analysis and implications for dispersion model chemistry methods using Las Vegas, Nevada near-road field measurements. Atmos. Environ. 165, 23–34. https://doi.org/10.1016/j.atmosenv.2017.06.027.

Kumar, A., Patil, R., Dikshit, A., Kumar, R., Brandt, J., Hertel, O., 2016. Assessment of impact of unaccounted emission on ambient concentration using DEHM and AERMOD in combination with WRF. Atmos. Environ. 142. https://doi.org/10.1016/j.atmosenv.2016.08.024.

Lloret, J., Carreño, A., Carić, H., San, J., Fleming, L.E., 2021. Environmental and human health impacts of cruise tourism: a review. Mar. Pollut. Bull. 173, 112979. https://doi.org/10.1016/j.marpolbul.2021.112979.

Ma, J., Yi, H., Tang, X., Zhang, Y., Xiang, Y., Pu, L., 2013. Application of AERMOD on near future air quality simulation under the latest national emission control policy of China: a case study on an industrial city. J. Environ. Sci. 25 (8), 1608–1617. https://doi.org/10.1016/S1001-0742(12)60245-9.

Maragkogianni, A., Papaefthimiou, S., 2015. Evaluating the social cost of cruise ships air emissions in major ports of Greece. Transp. Res. Part D: Transp. Environ. 36, 10–17. https://doi.org/10.1016/j.trd.2015.02.014.

Matacchiera, F., Manes, C., Beaven, R.P., Rees-White, T.C., Boano, F., Mønster, J., Scheutz, C., 2019. AERMOD as a Gaussian dispersion model for planning tracer gas dispersion tests for landfill methane emission quantification. Waste Manag. 87, 924–936. https://doi.org/10.1016/j.wasman.2018.02.007 New York, N.Y.

Mendoza-Lara, O.O., Arévalo-Mendoza, V., Villareal-Esquivel, C.G., Pérez-Castillo, A., Morales-González, A., 2021. Evaluación del modelo meteorológico WRF para la validación del modelo AERMOD. Tecnol. Cienc. Estud. Organ. 3 (1), 56–74. https://doi.org/10.56913/teceo.3.5.56-74.

Moctezuma Escamilla, D., Ignacio Sánchez, C.I., Aguila Sainz, A., 2022. Reporte de la calidad del aire. BCSicletos.

Mokhtar, M.M., Hassim, M.H., Taib, R.M., 2014. Health risk assessment of emissions from a coal-fired power plant using AERMOD modelling. Process Saf. Environ. Prot. 92 (5), 476–485. https://doi.org/10.1016/j.psep.2014.05.008.

Monbureau, E.M., Heist, D.K., Perry, S.G., Brouwer, L.H., Foroutan, H., Tang, W., 2018. Enhancements to AERMOD's building downwash algorithms based on wind-tunnel and embedded-LES modeling. Atmos. Environ. 179, 321–330. https://doi.org/10.1016/j.atmosenv.2018.02.022.

Murena, F., Mocerino, L., Quaranta, F., Toscano, D., 2018. Impact on air quality of cruise ship emissions in Naples, Italy. Atmos. Environ. 187, 70–83. https://doi.org/10.1016/j.atmosenv.2018.05.056.

National Centers for Environmental Prediction, National Weather ServiceNOAA, U.S. Department of Commerce, 2000. NCEP FNL Operational Model Global Tropospheric Analyses, Continuing From July 1999. Research Data Archive at the National Center for Atmospheric Research, Computational and Information Systems Laboratory. https://doi.org/10.5065/D6M043C6.

Nguyen, P.-N., Woo, S.-H., Kim, H., 2022. Ship emissions in hotelling phase and loading/unloading in Southeast Asia ports. Transp. Res. Part D: Transp. Environ. 105, 103223. https://doi.org/10.1016/j.trd.2022.103223.

NOM-022-SSA1-2019,2019NOM-022-SSA1-2019 , (2019).

NOM-023-SSA1-2021,2021NOM-023-SSA1-2021 , (2021).

Nunes, R.A.O., Alvim-Ferraz, M.C.M., Martins, F.G., Peñuelas, A.L., Durán-Grados, V., Moreno-Gutiérrez, J., Jalkanen, J.-P., Hannuniemi, H., Sousa, S.I.V., 2021. Estimating the health and economic burden of shipping related air pollution in the Iberian Peninsula. Environ. Int. 156, 106763. https://doi.org/10.1016/j.envint.2021.106763.

O'Shaughnessy, P.T., Altmaier, R., 2011. Use of AERMOD to determine a hydrogen sulfide emission factor for swine operations by inverse modeling. Atmos. Environ. 45 (27), 4617–4625. https://doi.org/10.1016/j.atmosenv.2011.05.061.

Pallis, P.L., 2017. Port risk management in container terminals. Transp.Res.Procedia 25, 4411–4421. https://doi.org/10.1016/J.TRPRO.2017.05.337.

Pan, X., 2011. In: Nriagu, J.O.B.T.-E.ofE.H. (Ed.), Sulfur Oxides: Sources, Exposures And Health Effects. Elsevier, pp. 290–296 https://doi.org/10.1016/B978-0-444-52272-6.00069-6.

Pandey, G., Sharan, M., 2019. Accountability of wind variability in AERMOD for computing concentrations in low wind conditions. Atmos. Environ. 202, 105–116. https://doi.org/10.1016/j.atmosenv.2019.01.017.

Páramo-Figueroa, V.H., 2019. Estado de la Calidad del Aire en México. Blog. https://www.gob.mx/inecc/es/articulos/estado-de-la-calidad-del-aire-en-mexico?idiom=es.

Perdiguero, J., Sanz, A., 2020. Cruise activity and pollution: the case of Barcelona. Transp. Res. Part D: Transp. Environ. 78, 102181. https://doi.org/10.1016/j.trd.2019.11.010.

Qi, N., Tan, X., Wu, T., Tang, Q., Ning, F., Jiang, D., Xu, T., Wu, H., Ren, L., Deng, W., 2022. Temporal and spatial distribution analysis of atmospheric pollutants in Chengdu-Chongqing Twin-City economic circle. Int. J. Environ. Res. Public Health 19 (7). https://doi.org/10.3390/ijerph19074333.

Reche, C., Tobias, A., Viana, M., 2022. Vehicular traffic in urban areas: health burden and influence of sustainable urban planning and mobility. Atmosphere. Vol. 13. https://doi.org/10.3390/atmos13040598.

Ruiz-Guerra, I., Molina-Moreno, V., Cortés-García, F.J., Núñez-Cacho, P., 2019. Prediction of the impact on air quality of the cities receiving cruise tourism: the case of the Port of Barcelona. Heliyon 5 (3), e01280. https://doi.org/10.1016/j.heliyon.2019.e01280.

Saha, S., Moorthi, S., Wu, X., Wang, J., Nadiga, S., Tripp, P., Behringer, D., Hou, Y.-T., Chuang, H., Iredell, M., Ek, M., Meng, J., Yang, R., Mendez, M.P., van den Dool, H., Zhang, Q., Wang, W., Chen, M., Becker, E., 2011. NCEP Climate Forecast System Version 2 (CFSv2) 6-hourly Products. Research Data Archive at the National Center for Atmospheric Research, Computational and Information Systems Laboratory. https://doi.org/10.5065/D61C1TXF.

Sarnelli, N.J., 2021. Apocalypse Ahoy: how the cruise industry boom is harming the world's oceans and problems with enforcing environmental regulations. Brooklyn Law Rev. 86 (3), 1035–1064.

Seangkiatiyuth, K., Surapipith, V., Tantrakarnapa, K., Lothongkum, A.W., 2011. Application of the AERMOD modeling system for environmental impact assessment of NO2 emissions from a cement complex. J. Environ. Sci. 23 (6), 931–940. https://doi.org/10.1016/S1001-0742(10)60499-8.

SEMARNAT, 2020. Monitoreo y evaluación de la Calidad del Aire. Consulta Temática. http://dgeiawf.semarnat.gob.mx:8080/ibi_apps/WFServlet?IBIF_ex=D3_R_AIRE01_12&IBIC_user=dgeia_mce&IBIC_pass=dgeia_mce#:~:text=Sistema-de-Monitoreo-de-Calidad,en-una-zona-o-región.

SINAICA, 2022. Sistema Nacional de Información de la Calidad del Aire. https://sinaica.inecc.gob.mx/ Issue 3.

SMN, 2022. Base de datos meteorológicos de las estaciones meteorológicas automáticas. https://smn.conagua.gob.mx/es/observando-el-tiempo/estaciones-meteorologicas-automaticas-ema-s.

Stefanidaki, E., Lekakou, M., 2014. Cruise carrying capacity: a conceptual approach. Res. Transp. Bus. Manag. 13, 43–52. https://doi.org/10.1016/j.rtbm.2014.11.005.

Universidad Autónoma de Baja California Sur, 2016. Inventario de emisiones para la ciudad de La Paz, Baja California Sur.

de Vries, W., 2021. Impacts of nitrogen emissions on ecosystems and human health: a mini review. Curr.Opin.Environ.Sci.Health 21, 100249. https://doi.org/10.1016/j.coesh.2021.100249.

WHO, 2016. Ambient Air Pollution: A Global Assessment of Exposure And Burden of Disease.

WHO, 2022. Ambient (outdoor) air pollution. https://www.who.int/news-room/fact-sheets/detail/ambient-(outdoor)-air-quality-and-health#:~:text=The-current-WHO-guideline-value,effects-of-gaseous-nitrogen-dioxide.

Zou, B., Zhan, F., Wilson, J., Zeng, Y., 2010. Performance of AERMOD at different time scales. Simul. Model. Pract. Theory 18, 612–623. https://doi.org/10.1016/j.simpat.2010.01.005.